JOURNAL OF MATERIALS SCIENCE **39** (2004) 6449– 6456

Recycling of magnesium alloy AZ91 scrap by a B_2O_3-containing flux

HONG TAO GAO,* GUO HUA WU, WEN JIANG DING, YAN PING ZHU
State Key Laboratory of Metal Matrix Composites, School of Materials Science and Engineering, Shanghai Jiao Tong University, Shanghai 200030, People's Republic of China
E-mail: hunterise@sohu.com; hunter@sjtu.edu.cn

A new flux was developed specially for recycling of scrap magnesium alloy AZ91 with high iron content. JDMJ in the flux could effectively remove inclusions from the recycled magnesium alloy and its proper addition was about 2.0 wt%. Excessive addition of the flux would result in flux inclusion in the recycled magnesium alloy. B_2O_3 in the flux made the iron concentration in the scrap magnesium alloy decrease from 0.044 wt% to about 0.002 wt% during recycling and its optimal addition was 0.3 wt% by Gaussian Fitting. The tensile properties of the recycled magnesium alloy were greatly improved by about 35%. Weight loss measurement, potentiodynamic study and pitting morphology examination revealed that the corrosion resistance of the recycled magnesium alloy was also greatly improved. The mechanisms of inclusion removing and iron reducing in the scrap magnesium alloy during recycling were discussed thermodynamically and formation of FeB was confirmed as the main reason for iron reducing in the recycled magnesium alloy AZ91 by XRD analysis.

1. Introduction

Magnesium is one of the lightest metals which makes the magnesium alloys extremely attractive for transport, aerospace and electronics applications [1, 2]. Magnesium alloys also have exceptional dimensional stability, high damping capacity and good fatigue resistance as well as excellent castability and workability. Because of these advantages, the demand for magnesium alloys has been increasing significantly since 1990's [3–6].

Increasing consumption of magnesium alloys entails an urgent need of the establishment of adequate recycling technology for these materials, as this will further reduce production cost and environmental degradation. Magnesium alloys are typical recyclable materials since they exhibit high recoverability from recycling. However, during processing and transporting contamination by impurities, iron in special, which can remarkably impair corrosion resistance of magnesium alloys [7–9], places a limitation on the recycling of magnesium alloys [10–13].

At present, disadvantages of the recycling techniques for magnesium alloys include complicated process, high cost and unsatisfactory result for magnesium alloys with high iron content. In order to avoid the disadvantages as above mentioned the author proposed the method that was refining magnesium melt with the new flux containing JDMJ (mainly chlorate), which was developed by Shanghai Jiao Tong University [14], and B_2O_3. JDMJ mainly remove non-metallic inclusions such as MgO and Mg_3N_2; B_2O_3 can react with iron and then reduce the iron concentration in magnesium alloys.

In the present experiment the effects of JDMJ and B_2O_3 on the inclusion content and the iron concentration of the recycled magnesium alloy AZ91 were investigated respectively. Then the tensile properties and the corrosion resistance of the recycled magnesium alloy were also studied.

2. Experimentals

2.1. Materials

Commercial magnesium alloy AZ91, which is the most widely used die casting magnesium alloy, was adopted in the present work. The scrap (wt%, Al: 9.26, Zn: 0.816, Mn: 0.191, Be: 0.0004, Fe: 0.0443, Cu: 0.0087, Si: 0.0262, Ni: 0.0008, Mg: Balance) contained casting sprues, runners, cuttings, and returned materials. The new flux was prepared in QM-ISP pebble mill with JDMJ (wt%, $MgCl_2$: 45, KCl: 25, NaCl: 20, others: 10) and chemical pure B_2O_3 ($\geq$98.0%).

2.2. Preparation

The magnesium alloy AZ91 scraps were decontaminated and dried before being melted in crucible electric resistance furnace under the protection of a mixed gas atmosphere of SF_6 (1 vol%) and CO_2 (bal.). The melt was treated by the new flux with different ratios of JDMJ and B_2O_3 additions shown in Tables I and II

*Author to whom all correspondence should be addressed.

TABLE I Flux ingredient (wt%)

	Flux ingredient	
Specimen code	JDMJ	B_2O_3
JB00000	0	0
JB05000	0.5	0
JB10000	1	0
JB15000	1.5	0
JB20000	2	0
JB25000	2.5	0
JB30000	3	0

TABLE II Flux ingredient (wt%)

	Flux ingredient	
Specimen code	JDMJ	B_2O_3
JB20000	2	0
JB20010	2	0.1
JB20015	2	0.15
JB20020	2	0.2
JB20025	2	0.25
JB20030	2	0.3
JB20035	2	0.35
JB20040	2	0.4
JB20045	2	0.45

at the temperature of 740°C. Then the melt was hold at the temperature for one hour and then poured into permanent molds (300°C) shown in Figs. 1 and 2. Tensile specimens with a gauge section of 25 mm × 6 mm × 2 mm and corrosion specimens with a gauge section of Φ35 mm × 5 mm were cut by electric spark machining from the ingots. The sludge that precipitated at the crucible bottom was collected after pouring.

2.3. Microstructural characterization

Statistical volume fractions of inclusions in metallographic specimens were measured by using Leco image software. First we observed the metallographic specimens by an OLYMPUS PME3 optical microscope, and then defined the inclusions as some color. Finally we selected 100 random fields, and Leco can output the area of the volume fraction of inclusions by color contrast.

Chemical composition (iron concentration) was ascertained with Inductively Coupled Plasma spectrum machine (ICP, IRIS Advantage 1000) produced by Thermo Jarrell Ash Company. Metallographs and corrosion photographs of specimens were observed by the optical microscope (OM, OLYMPUS PME3) and a scanning electron microscope (SEM, PHILIP SEM515). Compositions of inclusions were analyzed using an energy dispersive spectroscope (EDS) attached to the SEM. Phases in the sludge were ascertained by means of an X-ray diffractometer (XRD, Rigaku Dmax-rC).

2.4. Tensile properties

Tensile tests were carried out on a Zwick/Roell materials testing machine at a tensile speed of 0.5 mm/min.

2.5. Corrosion testing

2.5.1. Weight loss measurement

For constant immersion testing, the specimens were polished successively on finer grades of emery papers up to 1000 level. All the specimens were initially cleaned using the procedure of ASTM standard G-I-72. The polished and preweighted specimens were exposed to ASTM D1384-87 water (148 mg/l Na_2SO_4, 138 mg/l $NaHCO_3$ and 165 mg/l NaCl) saturated with $Mg(OH)_2$ (pH = 10.6) maintained at room temperature (25 ± 0.5)°C for various intervals of time, without stirring. The size of the samples ratio: volume of solution (ml) surface (cm^2) was set to 5. Final cleaning of the specimens at the end of the test was done by dipping in a solution of 15 wt% CrO_3 + 1 wt% $AgNO_3$ in 100 ml water at boiling condition for about 15 min. Consequently, the specimens were rinsed by cleaning in boiling water and dried in a stream hot air. The weights of the corroded specimens were measured after each experiment. The weight loss was calculated by the equation:

$$WL = \frac{W_0 - W_c}{SA}$$

where W_0 (mg) and W_c (mg) denote the weights of the specimens before and after immersion respectively. *SA* (cm^2) denotes the total surface area of each specimen.

2.5.2. Potentiodynamic polarization curve

The potentiodynamic polarization curve for each specimen was measured in a glass cell using a ZF potentiostat system with a scanning rate of 2 mV/s. The counter electrode was platinum, and a saturated calomel electrode (SCE) was used as reference. All potentials are referred to the SCE.

3. Results

3.1. Inclusions

Table III shows the statistical volume fractions of the inclusions in the recycled magnesium alloy by using

TABLE III Statistical volume fraction of inclusions in recycled magnesium alloy

Specimen code	Number of fields	Total area of fields/mm^2	Maximum volume fraction (%)	Minimum volume fraction (%)	Average volume fraction (%)
JB00000	100	1.4	6.53	0.95	2.06
JB10000	100	1.4	1.26	0.29	1.08
JB20000	100	1.4	0.67	0.12	0.26
JB30000	100	1.4	0.96	0.34	0.51

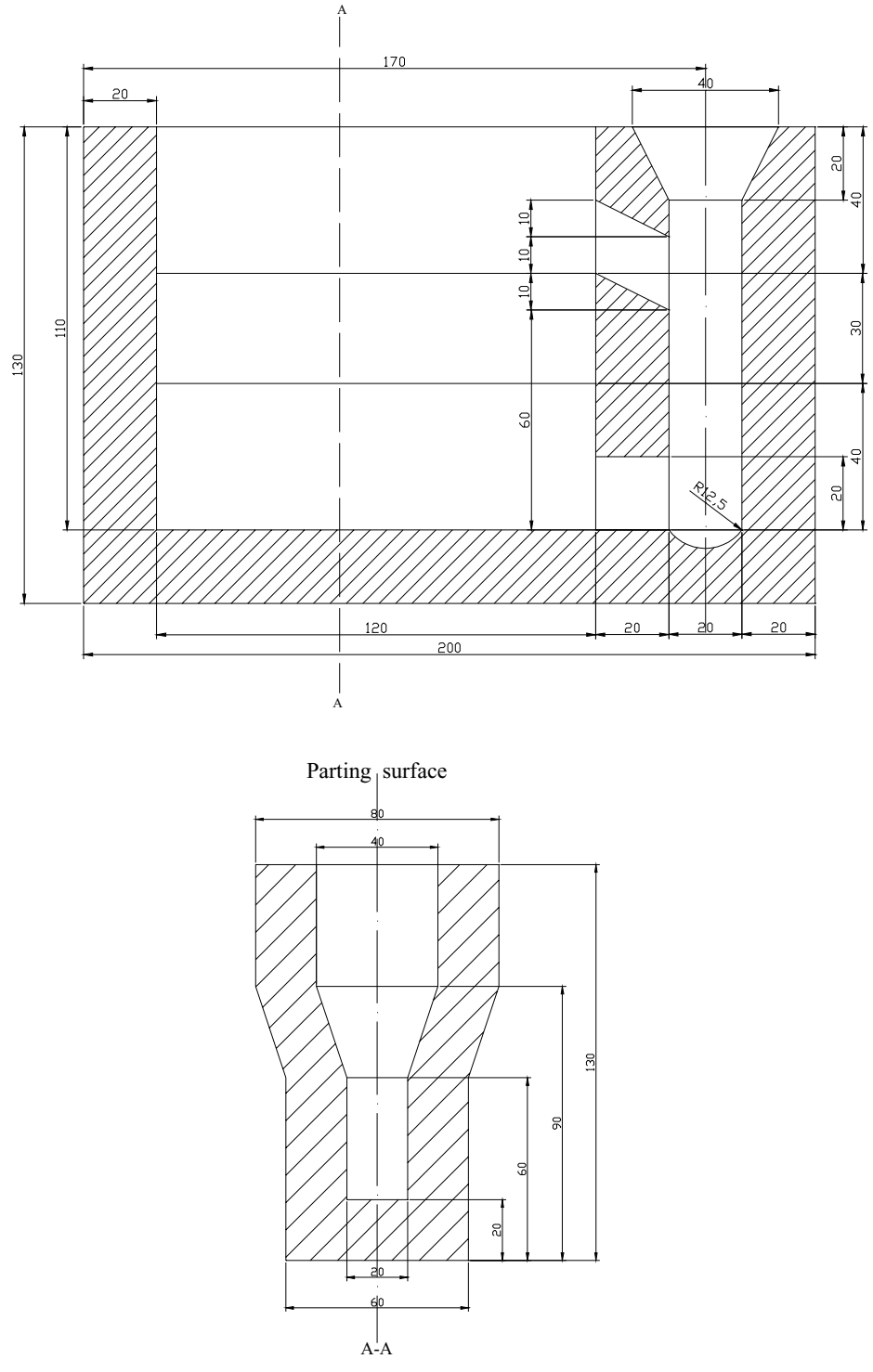

Figure 1 Permanent mold of tensile samples.

Leco image software. It can be seen that the average volume fraction of the inclusions in the recycled specimens decreases with the increasing JDMJ addition in the flux. However, it increases from 0.26 to 0.51% when the JDMJ addition increases from 2.0 to 3.0 wt% in the flux. Fig. 3 is the typical optical micrographs of the recycled specimens JB00000, JB10000, JB20000 and JB30000.

As can be seen in Table III and Fig. 3 it is notable that there are more inclusions in the specimen JB30000 than the specimen JB20000 though more JDMJ are added in the flux for the former than the later during recycling. In further research flux inclusions are found in the specimen JB30000 by SEM and EDS. Fig. 4 is the morphologies of the flux inclusions and their EDS analysis results. It is certain that the inclusions showed are just flux inclusions because there are Cl and F elements detected according to their EDS results. Therefore, excessive flux can be involved in magnesium melt and then result in flux inclusions during recycling.

3.2. Iron concentration

Table IV shows the chemical composition of the recycled magnesium alloy. Fig. 5 shows B_2O_3dependence of the iron concentration in the recycled magnesium

TABLE IV Chemical composition of the recycled magnesium alloy

	Chemical composition (wt%)								
Specimen code	Al	Zn	Mn	Be	Fe	Cu	Si	Ni	Mg
JB20000	9.23	0.811	0.183	0.0003	0.0441	0.0082	0.0251	0.0008	Balance
JB20020	9.28	0.806	0.186	0.0003	0.0043	0.0076	0.0257	0.0007	Balance
JB20030	9.19	0.812	0.187	0.0004	0.0017	0.0079	0.0253	0.0008	Balance
JB20045	9.32	0.819	0.192	0.0003	0.0011	0.0081	0.0261	0.0008	Balance

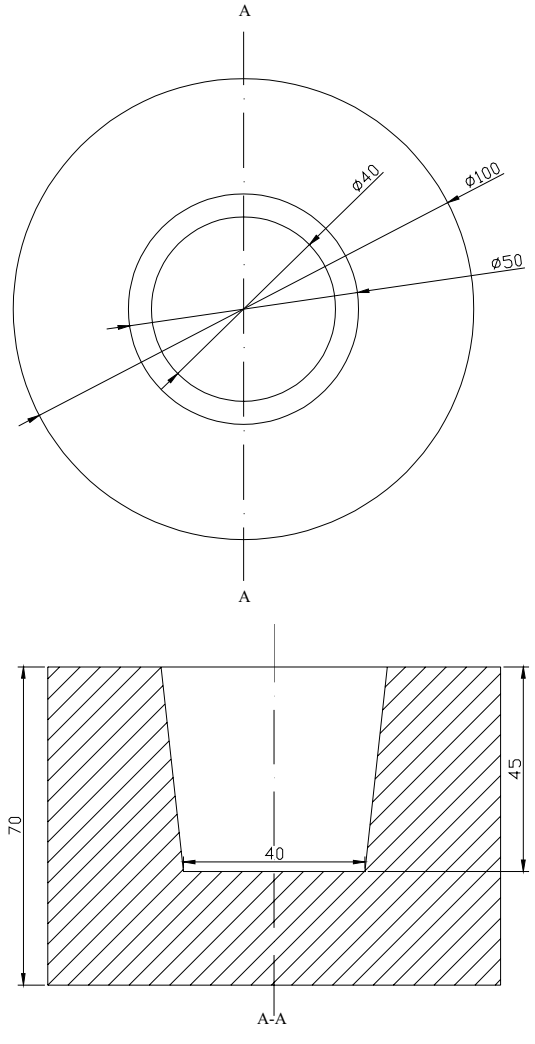

Figure 2 Permanent mold of corrosion samples.

alloy. With increasing B_2O_3 addition in the flux, the iron concentration in the recycled specimens decreases sharply at the beginning and then remains only a little changeable when it reaches 0.002 wt%. The equation can be obtained by Gaussian Curve Fitting:

$$y = 0.00138 + 0.047e^{-50.6768\times(x+0.04377)^2}$$

The limit value of y is 0.00138, and x is 0.3 when the fit deviation is controlled within 1%. The degree of confidence R^2 is 0.99971. Therefore, in the experiment the limit value of the iron concentration in the recycled magnesium alloy is decided as 0.00138 wt% and the optimal addition of B_2O_3 in the flux is about 0.3 wt%.

There are complicated physical and chemical reactions between magnesium melt and the flux in the process of recycling. During the reaction the thermodynamic potential becomes weaker with decreasing iron concentration in magnesium melt till thermodynamic equilibrium. Therefore, the iron concentration does not change greatly even though more B_2O_3 is added in the flux. Dynamical model for iron atoms transferring through magnesium melt-flux boundary, which is given in Fig. 6, illustrates that there is larger difficulty for iron atoms in transferring through magnesium melt-flux boundary with decreasing iron concentration in magnesium melt according to the first Fick diffusion law. In Fig. 6, C_1 and C_2 denote the iron concentrations at the melt/boundary interface and the boundary/flux interface respectively.

3.3. Tensile properties

The tensile properties of the recycled magnesium alloy are shown in Fig. 7. At the beginning, the tensile properties of the recycled specimens improve significantly with increasing JDMJ addition in the flux. And the improving extent is about 35%. Both the ultimate strength and the elongation reach the maximum values at the critical addition 2.0 wt% of JDMJ in the flux. And then both of them go down when the JDMJ addition is above 2.0 wt%. It is known that with increasing JDMJ addition in the flux the inclusions in the recycled magnesium alloy decrease, thus dissevering the magnesium matrix more slightly, which improves the tensile properties of the recycled magnesium alloy. As to the declination of the tensile properties after 2.0 wt% of JDMJ addition, it is attributed to the increasing flux inclusions in the recycled magnesium alloy.

3.4. Corrosion resistance

The corrosion rates of the recycled magnesium alloy after immersion in the testing solution for different time are illustrated in Fig. 8. It can be seen that the weight loss of each recycled specimen increases with increasing immersion time. For immersion time of 72 h the weight loss of the specimen treated by 0.45 wt% B_2O_3 in the flux is only 0.5 mg/cm^2 as contrast to 53 mg/cm^2 for the specimen treated by 0% B_2O_3 in the flux. Therefore the conclusion can be drawn that the new flux is effective on improving the corrosion resistance of the recycled magnesium alloy.

The potentiodynamic polarization curves for the specimens JB20000, JB20020, JB20030 and JB20045 are shown in Fig. 9. It can be seen that the polarization curves for all the specimens are not symmetrical between their anodic and cathodic branches. Much

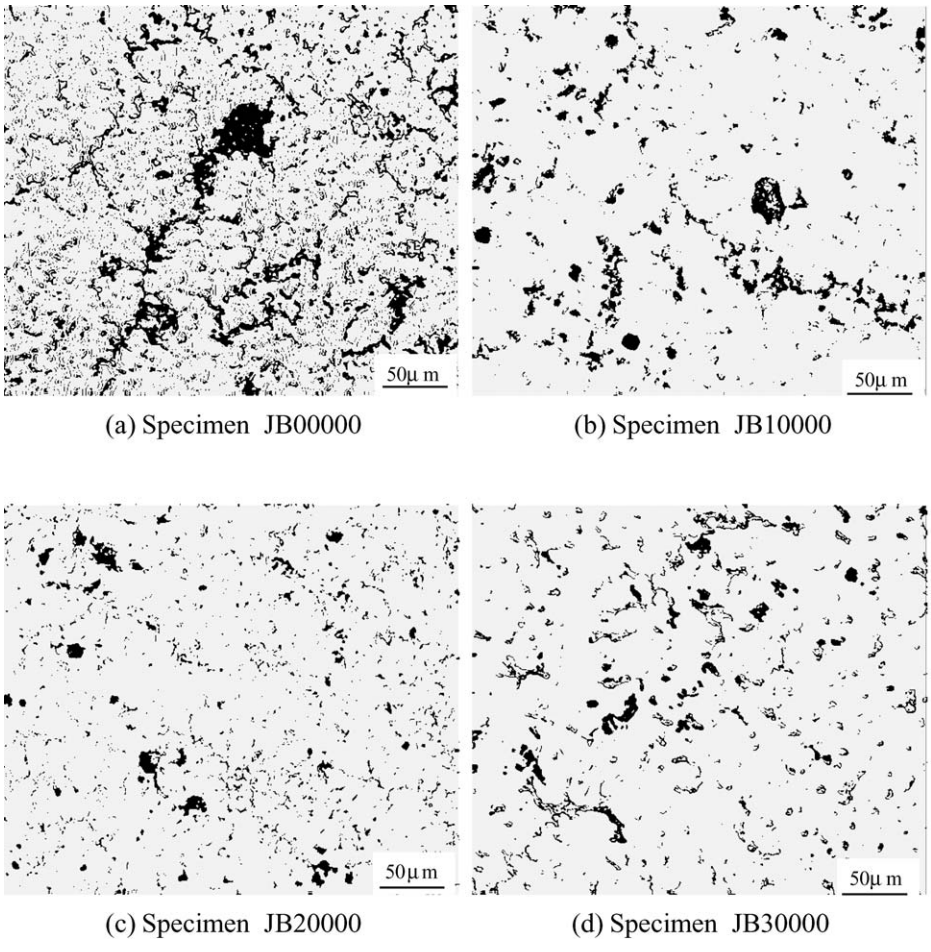

(a) Specimen JB00000 (b) Specimen JB10000

(c) Specimen JB20000 (d) Specimen JB30000

Figure 3 Metallographic photographs of recycled magnesium alloy.

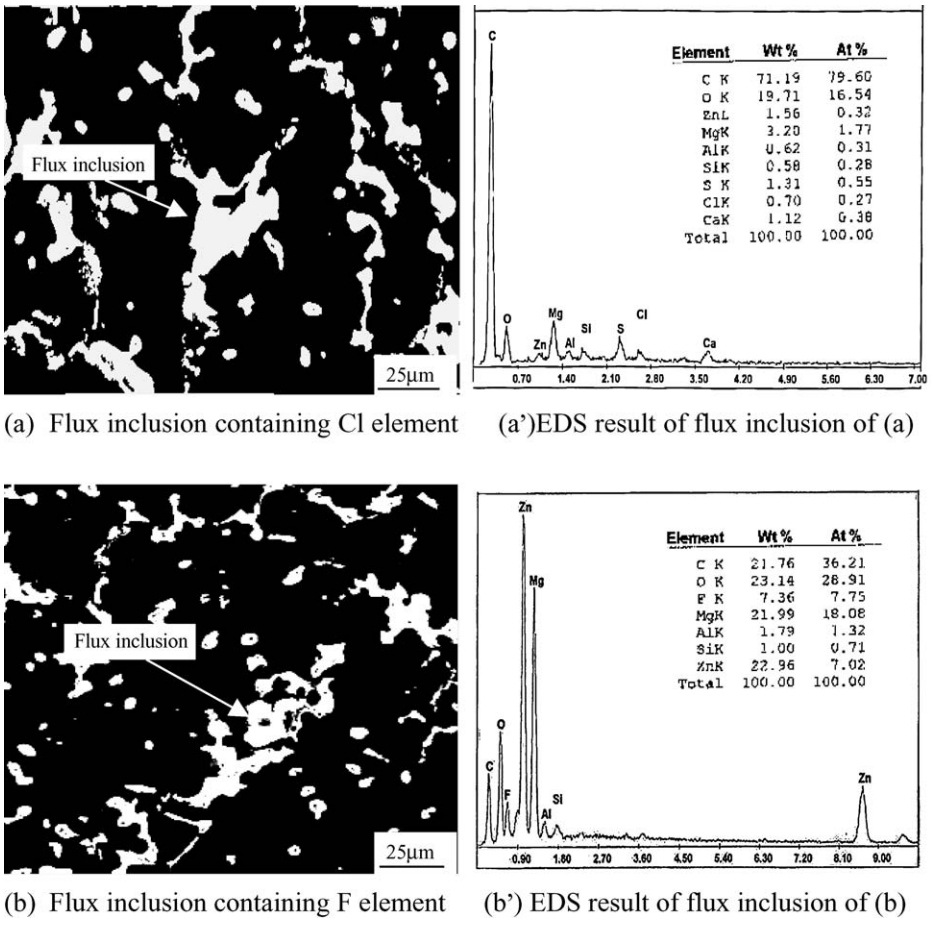

(a) Flux inclusion containing Cl element (a')EDS result of flux inclusion of (a)

(b) Flux inclusion containing F element (b') EDS result of flux inclusion of (b)

Figure 4 SEM micrographs of flux inclusions and their EDS results.

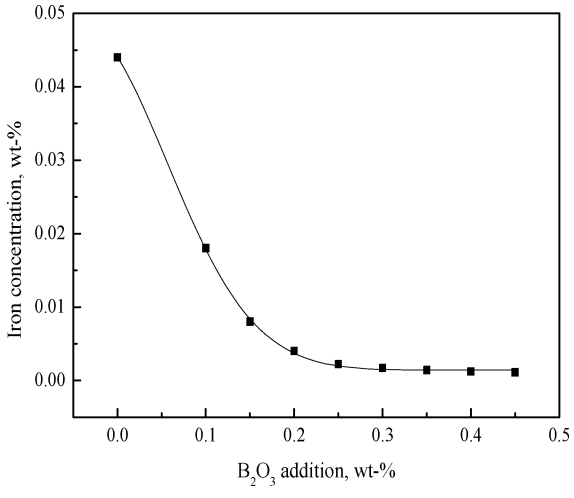

Figure 5 B_2O_3 dependence of iron concentration in recycled magnesium alloy.

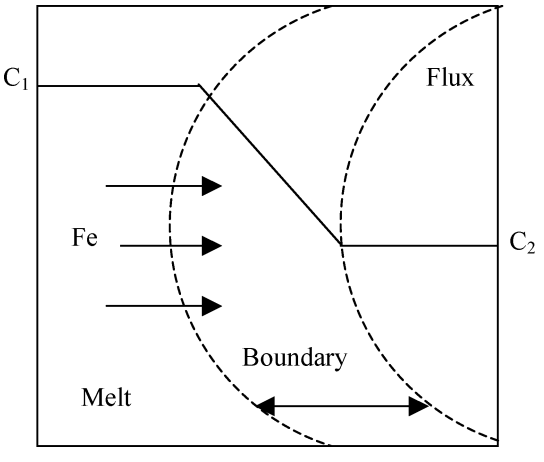

Figure 6 Schematic illustration of iron atoms transferring through melt-flux boundary.

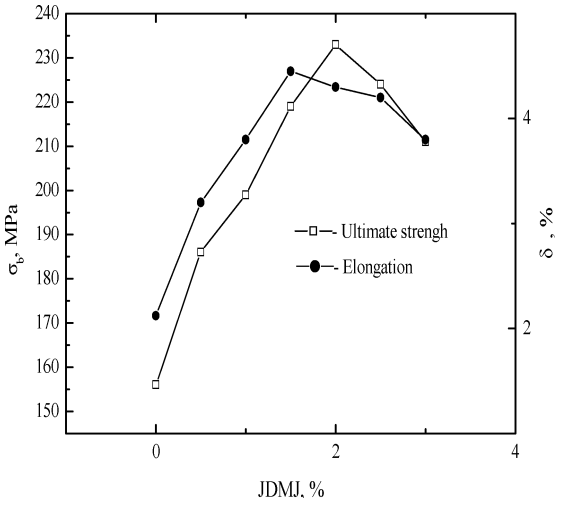

Figure 7 Relationship between JDMJ addition and tensile properties of recycled magnesium alloy.

sharper changes in current density vs. applied potential are observed in the anodic polarization branches than in the cathodic polarization branches. And the corrosion potential increases in the following order: specimen JB20045 < specimen JB20030 < specimen JB20020 < specimen JB20000. Furthermore, the cathodic current densities are much higher for specimens JB20000 and JB20020 than specimens JB20030 and JB20045 at all potentials. All the differences are owing to the different iron concentrations in the recycled magnesium alloy treated by the flux with different B_2O_3 additions.

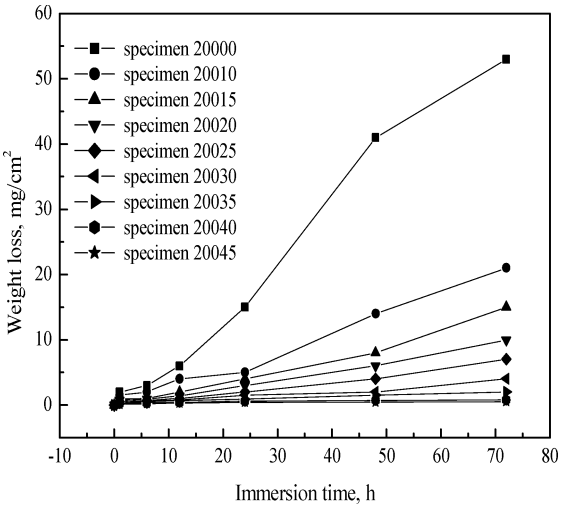

Figure 8 Corrosion rates of recycled magnesium alloy.

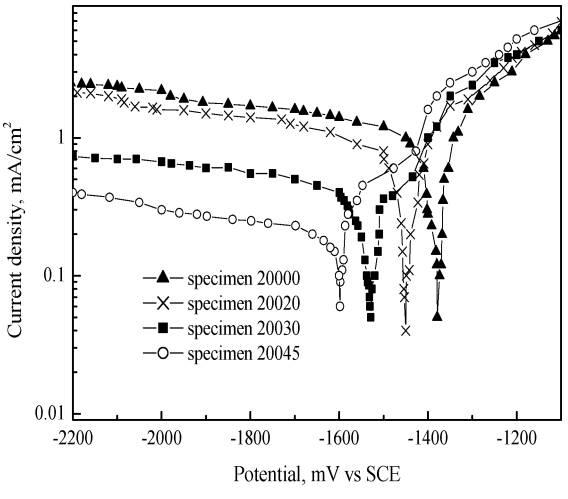

Figure 9 Polarization curves for specimens JB20000, JB20020, JB20030 and JB20045.

The morphological characteristics of the corroded surfaces for the specimens JB20000, JB20020, JB20030 and JB20045 after being immersed in the testing solution for 72 h are shown as Fig. 10. It can be seen that there are corrosion pits homogeneously distributed on the surface of each specimen. The difference lies in the fact that the pits become denser and deeper in the following order: specimen JB20045 < specimen JB20030 < specimen JB20020 < specimen JB20000.

It is known that B_2O_3 in the flux can remarkably decreases the iron concentration in the recycled magnesium alloy. Because of low solubility in magnesium most iron precipitates and scatters on magnesium matrix, which can remarkably impair corrosion resistance of magnesium alloy. Reducing amount of iron in the recycled magnesium alloy, which is attributed to B_2O_3, leads to the increasing corrosion resistance for the recycled magnesium alloy.

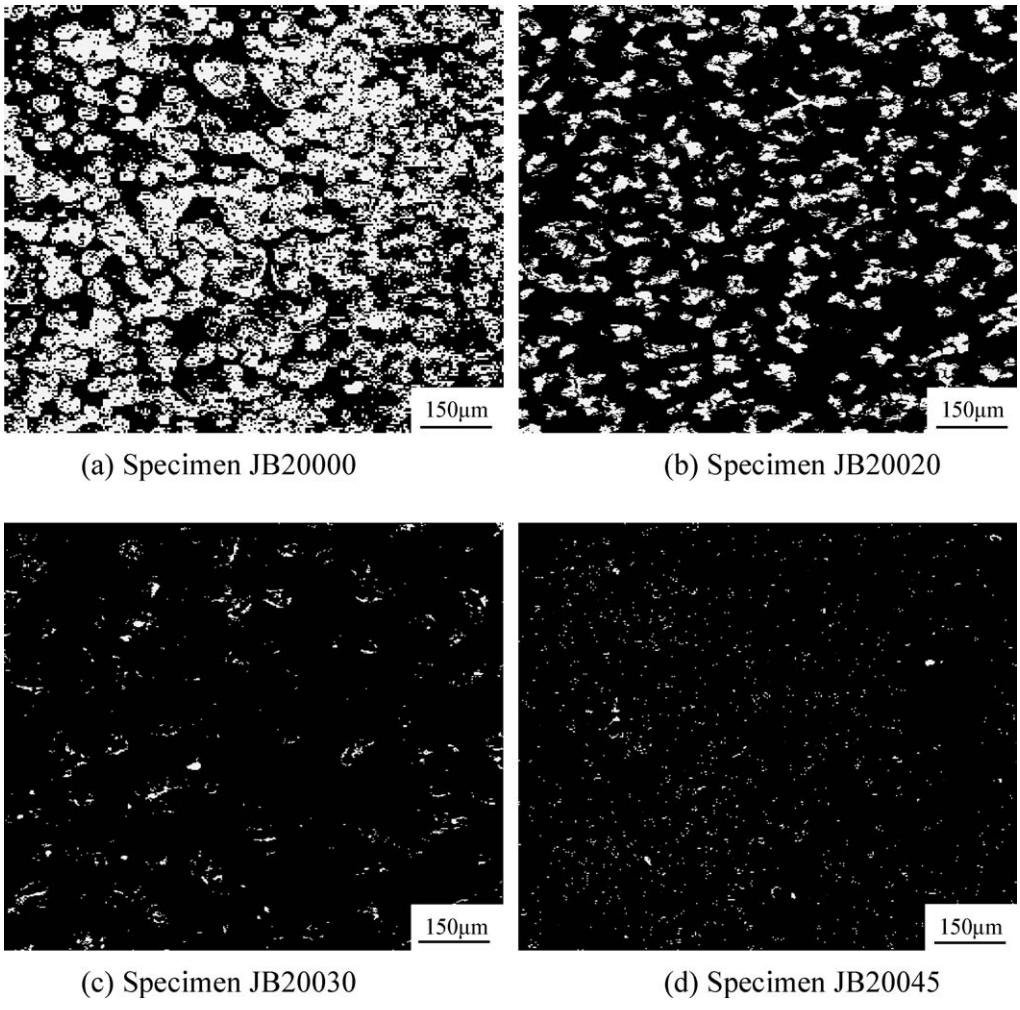

(a) Specimen JB20000 (b) Specimen JB20020

(c) Specimen JB20030 (d) Specimen JB20045

Figure 10 Photographs of corroded surfaces for specimens JB20000, JB20020, JB20030 and JB20045 after immersion in testing solution for 72 h.

4. Discussion

It is known that there are many kinds of inclusions in recycled magnesium alloy in which MgO is in the majority [15, 16]. Most of them are wetted by $MgCl_2$ and KCl in the new flux [17, 18]. And some of them might react with $MgCl_2$ and form stable or unstable complex substance illustrated as follows:

$$MgO + MgCl_2 \longrightarrow MgCl_2{\cdot}MgO$$

$$5MgO + MgCl_2 \longrightarrow 5MgCl_2{\cdot}MgO$$

The Gibbs free energy of inclusions absorbed by the flux from magnesium melt is expressed as:

$$\begin{aligned}\Delta G &= \sigma_{\text{flux}-\text{inclusion}} - \sigma_{\text{melt}-\text{inclusion}} \\ &= \sigma_{\text{melt}} \cos\theta_{\text{melt}-\text{inclusion}} - \sigma_{\text{flux}} \cos\theta_{\text{flux}-\text{inclusion}} \\ &= \sigma_{\text{melt}-\text{flux}} \cos\theta_{\text{flux}}^{\text{melt}-\text{inclusion}}\end{aligned}$$

where $\theta_{\text{melt}-\text{inclusion}}$ and $\theta_{\text{flux}-\text{inclusion}}$ are wetting angles between inclusions and magnesium melt, the flux respectively; $\theta_{\text{flux}}^{\text{melt}-\text{inclusion}}$ is the wetting angle between inclusions and magnesium melt in the flux.

As can be seen in the above formula, ΔG will be more negative with decreasing $\sigma_{\text{melt}-\text{flux}}$ and it means easier for inclusions transferring from magnesium melt to the flux. Fluoride addition in the flux, which reduces the interfacial tension between magnesium melt and the flux, is helpful for inclusions removing from magnesium melt [19].

As to iron reducing in the recycled magnesium alloy during recycling, thermodynamic analysis is done by using the thermodynamic data [20, 21]:

$$B_2O_3(s) + 3Mg(l) = 3MgO(s) + 2B(s) \quad (1)$$

$$\Delta G_1^0 = -1828710 + 106.16T$$

$$B(s) + Fe(l) = FeB(s) \quad (2)$$

$$\Delta G_2^0 = -93300 + 18.07T$$

$$B_2O_3(s) + 3Mg(l) + 2Fe(l) = 3MgO(s) + 2FeB(s) \quad (3)$$

where s, l and g represent solid, liquid and gas respectively.

The standard Gibbs free energy of the reaction (3) is calculated:

$$\begin{aligned}\Delta G_3^0 &= \Delta G_1^0 + \Delta G_2^0 \times 2 = -2015310 + 142.3T \\ &= -1972905 \text{ (J/mol)} < 0 \quad (4)\end{aligned}$$

ΔG_3^0 is negative at the standard state (1 atmosphere and 298 K), indicating that the reaction (3) is spontaneous thermodynamically. Therefore, FeB can come

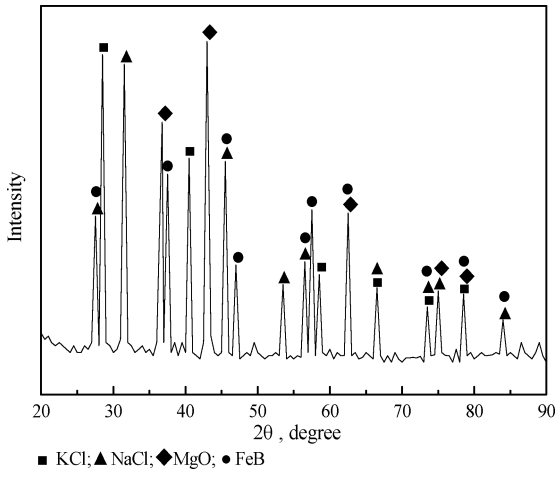

Figure 11 X-ray diffraction spectrum of the sludge.

into being in the magnesium alloy melt during the reaction. Furthermore, the reaction product FeB (its melting point is 1650°C) [21] settles down in course of recycling, which is confirmed by the XRD result of the melting sludge showed in Fig. 11.

5. Conclusions

(1) The average volume fraction of inclusions in the scrap magnesium alloy AZ91 greatly decreases during recycling by the new flux. The proper addition of JDMJ in the flux is about 2.0 wt% and more addition than this value can result in flux inclusion in the recycled magnesium alloy.

(2) B_2O_3 in the flux, which is proved to be effective on reducing iron in magnesium alloy, makes the iron concentration in the scrap magnesium alloy decrease from 0.044 wt% to about 0.002 wt% and its optimal addition is 0.3 wt% by Gaussian Fitting.

(3) The tensile properties of the recycled magnesium alloy increase by about 35%. And excessive flux can lead to decreasing tensile properties of the recycled magnesium alloy owing to appearance of flux inclusion.

(4) Weight loss measurement, potentiodynamic study and pitting morphology examination reveal that corrosion resistance of the recycled magnesium alloy is greatly improved.

(5) The mechanisms of inclusion removing and iron reducing in the magnesium alloy during recycling with this new flux are discussed thermodynamically and formation of FeB is confirmed as the main reason for iron reducing by XRD analysis.

Acknowledgement

The present study is funded by the National High Technology R&D Program of China (863 Plan: 2002AA331120) from the Ministry of Science and technology of the People's Republic of China.

References

1. C. B. JOSEPH, *Light Metal Age* **59**(8) (2001) 103.
2. H. FURUYA, N. KOGISO, S. MATUNAGA and K. SENDA, *Mater. Sci. Forum* **350** (2000) 341.
3. E. B. ROBERT, *Light Metal Age* **54**(9/10) (1996) 66.
4. R. BROWN, *ibid.* **58**(9/10) (2000) 54.
5. R. P. PAWLEK and R. B. BROWN, *ibid.* **59**(8) (2001) 50.
6. E. B. ROBERT, *ibid.* **61**(1/2) (2003) 53.
7. T. HAITANI, Y. TAMURA, T. MOTEGI, N. KONO and H. TAMEHIRO, *Mater. Sci. Forum* **419–422** (2003) 697.
8. J. D. HANAWALT, *Transaction AIME* **147** (1942) 279.
9. M. INOUE, M. IWAI, K. MATUZAWA, S. KAMADO and Y. KOJIMA, *J. Jpn. Inst. Light Met.* **48**(6) (1998) 257.
10. Y. CHINO, A. YAMAMOTO, H. IWASAKI, M. MABUCHI and H. TSUBAKINO, *Mater. Sci. Forum* **419–422** (2003) 671.
11. M. INOUE, M. IWAI, K. MATSUZAWA, S. KAMADO and Y. KOJIMA, *ibid.* **419–422** (2003) 691.
12. M. INOUE, M. IWAI, S. KAMADO, Y. KOJIMA, T. ITOH and M. SUGAMA, *Trans. Mater. Res. Soc. Jpn.* **24** (1999) 349.
13. K. KOICHI, N. KOUTA and K. MOTONOBU, *Mater. Trans.* **43** (2002) 2516.
14. C. ZHAI, W. DING, X. XU, Z. DENG and Z. YU, *Spec. Cast. Nonferr. Alloys* **4** (1997) 48.
15. G. H. ANDREW, A. M. BARRY and E. M. WILLIAM, *Light Metal Age* **54**(7/8) (1996) 6.
16. H. HENRY and L. ALAN, *JOM* **10** (1996) 47.
17. B. S. TERRY and P. GRIEVESON, *ISIJ International* **33** (1993) 166.
18. R. XU, "Magnesium Metallurgy" (Chinese) (Metallurgy Industry Press, Beijing, 1993) p. 257.
19. X. ZENG, Q. WANG and W. DING, *Light Alloy Proc. Techn.* **27** (1999) 5.
20. Y. LINAG, Y. CHE and X. LIU, "Handbook of Inorganic Thermodynamic Data" (North-East University Press, Shenyang, 1993) p. 458.
21. E. T. TURKDOGAN, "Physical Chemistry of High Temperature Technology" (Academic Press, New York, 1980) p. 25.

Received 29 October 2003
and accepted 2 June 2004